Impacts of buoyancy effects on the mixing at river confluences

E Dureuil, J Le Coz, Louis Gostiaux, E Mignot, Nicolas Riviere, Patrick Boyer

Impacts of buoyancy effects on the mixing at river confluences

E. Dureuil & J. Le Coz
INRAE, UR Riverly, River Hydraulics Group - Villeurbanne - France

L. Gostiaux & E. Mignot & N. Riviere
Laboratoire de Mécanique des Fluides et d'Acoustique - INSA Lyon, CNRS, Ecole Centrale de Lyon, Universite Claude Bernard Lyon 1, LMFA, UMR5509, 69621, Villeurbanne France

P. Boyer
Institut de Radioprotection et de Sûreté Nucléaire (IRSN), PSE/SRTE/LRTA, CE-Cadarache - France

ABSTRACT: Two concurrent phenomena govern the mixing pattern and efficiency at river confluences: the turbulent diffusion and the dispersion due to secondary currents. This dispersion may be caused, for example, by a strong momentum or density ratio among both inflows or a step at one inflow. The dominant type of mixing affects the length necessary for the good mixing hence, the ecological conditions and the water uses downstream of the confluence. The main goal of this publication is to present a way of visualizing the mixing pattern downstream a confluence, to identify the mixing interface and evaluate both phenomena. This methodology is applied to field measurements taken in various natural and man-made confluence configurations.

Keywords: density current, diffusion, dispersion, mixing, confluences

1 INTRODUCTION

1.1 *Context and state of the art*

In the fluvial continuum description, the rivers come into contact at confluences. These confluences can be described as a water supply into the main river. This supply can be artificial, and in this case it is almost always polluted (for example: a thermal outflow of a nuclear powerplant), or natural at a river confluence. In both cases, the water from each tributary has different intrinsic characteristics depending on geographical or hydrological conditions, and/or on industrial operations. In particular, the two flows often exhibit a difference in density and velocity as they merge. The density gradient is mainly caused by a temperature, suspended matter or salinity difference between the two flows so that the heavier flow passes under the lighter one (Pouchoulin et al. 2020). At the confluence, a gravity current tilts the mixing interface between the two rivers, and acts as a lock-exchange flow (Cheng and Constantinescu 2022), i.e as when two fluids of different densities are initially separated by a vertical gate and the gate is rapidly removed: the heavier (denser) fluid moves horizontally underneath the lighter fluid and generates a recirculating motion in the cross-section. As for all secondary motion, the lock exchange process is often referred to dispersion.
The other main process that contributes to the mixing of the two fluids is the turbulent diffusion caused by the velocity difference at the interface between the inflows.
As for a strong momentum ratio (Jiang et al. 2022), a gravity current generally increases the mixing efficiency. Consequently, the maximum mixing efficiency occurs as the main inflow is the coldest, and therefore, the heaviest (Lane et al. 2008). Also, the difference of inflow velocities impacts the transverse mixing coefficient by increasing the turbulent diffusion, and directly the length necessary for a good mixing (L_m). This length is defined as the concentration in a transverse profile with a concentration deviation lower than $\pm 5\%$ (Fischer 1979, Herrero et al. 2018) or ± 2 to 10% (Rutherford 1994). The mixing is then defined as "slow" for a value of dimensionless

length (with W : the river width), $L_m/W > 100$, and rapid, for $L_m/W < 10$ (Lane et al. 2008). One challenge that arises at a given confluence is to assess the relative contribution to the mixing from the dispersion and turbulent diffusion processes. To do so, previous authors proposed to use dimensionless numbers, such as the Gamma parameter "γ" (White and Helfrich 2013), the Densimetric Froude number "FrD" used by some authors (Horna-Munoz et al. 2020; Duguay et al. 2023), and the Richardson number, which is simply the opposite of the Densimetric Froude number.

1.2 *Scientific issue*

Currently, the quantification of the strength of a density effect in cross-section, and so, the description of "strong" or "weak" density effects remains qualitative without any consensus of how to calculate and quantify it. The existing dimensionless numbers listed above are somehow efficient for quantifying the global density effects on the mixing, but there remain a problem of consensus on where, or how terms are defined. For example, Horna-Munoz et al. (2020) state that when the Densimetric Froude number is smaller than 4, density effects are strong, and when this number is higher than 10, the mixing is dominated by turbulent diffusion induced by the shear. White and Helfrich (2013) state that when the Gamma parameter is lower than 1, then there are weak density driven effects, and strong gravity current when it is greater than 1.
The Gamma parameter is calculated as :

$$\gamma = \frac{5L_u(gH\Delta\rho^*)^{1/2}}{H|U_{main} - U_{trib}|} \tag{1}$$

where L_u: Length scale for the horizontal shear layer (m), g: Gravitationnal acceleration (m^2/s), H: Depth(m), $\Delta\rho*$: Relative density difference(kg/m^3), U_{main}: Main river velocity (m/s), U_{trib}: Tributary river velocity (m/s)

A limitation for the use of the Gamma parameter is that it is proportional to L_u, the scale required to establish the stratification, corresponding to a horizontal orientation of the mixing layer in cross-section, which increases with distance from the confluence. Pouchoulin et al. 2020, applied this parameter to their data by making a questionable hypothesis. It was assumed that $L_u = H$. In this case L_u was constant and equal to 9.2m. In the case 1, where there was a stratification, γ was equal to 330. In the other 2 cases, where density effects were weak, γ was closer to 1. In the case 2, the value was 1.3 because the density difference was negligible and there was mixing solely dominated by diffusion. In the third case the value of this number is 2.2, and this is where there was the observation of a weak stratification effects. This number was also applied by other authors (Ramón et al. 2013). In the four cases from these authors, the stratification effects increase when γ increases. And in the case of ibid., the value is 6.4 when the mixing is dominated by diffusion.

The same is true for the Densimetric Froude number:

$$FrD = \frac{U_0}{\sqrt{g'D}} \qquad with \qquad g' = g(\rho_1 - \rho_2)/\rho_1 \tag{2}$$

where g' is the reduced gravity, g is the gravitational acceleration, ρ_1 and ρ_2 are the densities of the denser tributary and the lighter tributary respectively. U_0 is the "bulk velocity", and D is the "characteristic depth" (Rhoads 2020). This leaves too many ambiguous interpretations and therefore, some difficulties remain in applying this number to predict the diffusion/dispersion relative contributions to the mixing. These confusions have been demonstrated in a recent work (Duguay et al. 2022b). For example, Horna-Munoz et al. (2020) states that when the Densimetric Froude number is less than 10, the density effects are large. However, in this same article, the authors expose a case where FrD = 4.9 with weak density effects, and another where FrD = 1.6 with strong density effects.

The Densimetric Froude number was calculated for each flow configuration and associated with qualitative description of the density effect by each author. The figure 1 intends to relate the value of FrD with the efficiency of lateral mixing downstream from a confluence, according to the conclusions raised in the papers of the literature, but it remains imprecise and only based on the qualitive description by each author (Duguay et al. 2023; Dong et al. 2023; Xu et al. 2022;

Jiang et al. 2022; Duguay et al. 2022a; Cheng and Constantinescu 2022; Horna-Munoz et al. 2020; Pouchoulin et al. 2020; Cheng and Constantinescu 2019; Gualtieri et al. 2019; Herrero et al. 2018; Lane et al. 2008). No clear threshold values of FrD could be found.

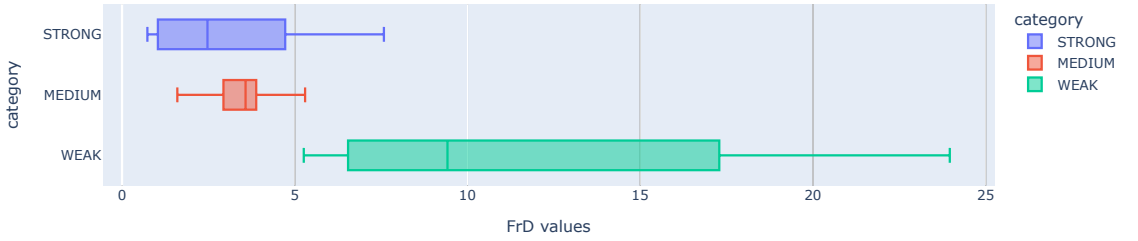

Figure 1.: Densimetric Froude number values corresponding to qualitative category description of density effect. These descriptions have been classified based on 47 cases in 12 publications, and our field measurements. The lines on the box plots represent the median.

1.3 *Objectives*

A problem in defining dimensionless numbers that evaluates the ratio of 1. dispersion caused by density effects & 2. turbulent diffusion was shown, so that, the main question is: "Is it possible to have a unique and reproducible measurement method to visualize the evolution of the mixing downstream of a confluence, based on field measurements, and to associate dimensionless numbers?". A method allowing the vizualisation of the mixing interface evolution along sections downstream is presented. Eight field experiments were performed until now. In the majority of cases, a gravity current strongly impacts the mixing, but in few cases, the mixing is dominated by the turbulent diffusion induced by the shear. To develop and demonstrate the proposed method, field measurements were performed at 2 river confluences and thermal outflows of nuclear power-plants (NPP) with contrasting hydrodynamics and density conditions. On this part, two different results are presented. The April case at Rhône-Saône confluence, which corresponds to a mixing dominated by dispersion induced by a strong gravity current, and the October case at Rhône-Bugey confluence which represents a mixing dominated by a diffusion. Finally, the Densimetric Froude number FrD, and the Gamma parameter γ are computed and compared among 8 field experiments.
The following sections describe the two different site locations, and the methods used to take samples and process data. The second part presents two mixing interface observations depending different hydrological cases. The last part is dedicated to the discussion of results obtained, with a conclusion on this study, then a description of the future work to be carried out.

2 METHODS AND DATA

2.1 *Locations*

8 field campaigns were carried out: 19 th December 2022 Rhône-Saône confluence; 4 th January 2023 Rhône-Arve confluence; 11 th April 2023 Rhône-Arve confluence; 12 th April 2023 Rhône-Saône confluence; 13 th July 2023 Rhône-Saône confluence; 21 th July 2023 Rhône-Saône confluence; 5 th October 2023 Rhône-Saône confluence; and 10 th October 2023 Rhône-Bugey confluence. Measurements presented below were taken at one river confluence, and one thermal outflow.

The Rhône-Saone confluence has an angle of 30° and Pouchoulin et al. (2020) have already made measurements on this site. It exhibits gravity currents inverted depending on the season because the Saone River is warmer in summer but colder in winter. The measurement length from the apex is about 2 km, limited by a harbour and a dam downstream. The Bugey NPP is located northeast of Lyon. The water used to cool the reactors is discharged into the river with a thermal

gradient forming a 20° angle confluence. Previous measurements revealed that the mixing seems dominated by the turbulent diffusion even if large density gradients exist due to the termal outflow and Rhône River temperature difference (ASN 2022).

2.2 *Field experiments method*

To start the measurements, the discharge, 3D velocity field, and the water conductivity / temperature of both inflows is first measured in one section of each tributary. The same procedure is applied downstream of the confluence along 4 to 8 sections the same day, depending on the available time (figures 4 and 5). The measurement protocol allowing to scan the evolution of the mixing interface is inspired by an existing method (Pouchoulin et al. 2020), but some improvements were made. A boat is borded with a DGPS (Differential Global Positioning System), and an ADCP (Acoustic Doppler Current Profiler) model TRDI Rio Grande 1200 kHz. Two line ropes are hung under the boat, and on each line rope, six couple of "DIVER" pressure probes, and "HOBO" conductivity/temperature probes are hooked and spaced 1 meter apart. A weight of 4 kg attached to the end of each garland helps limit the drag. A laptop with "WinRiver II" sofware is used to record measurements during field experiments. For each section, the data is averaged over 4 to 6 cross- section crossings. The poistion of cross-section are represented as X/W with X: Downstream length from the apex (m), and W : width (m).

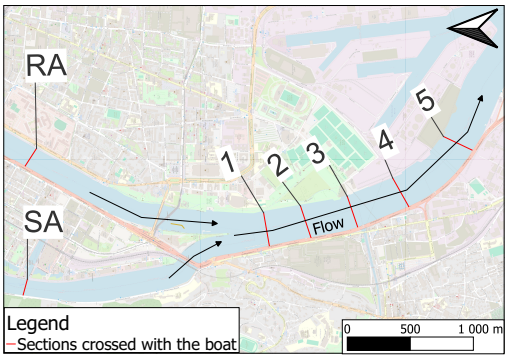

(a) Figure 2.a: Measurement cross-sections on Rhône-Saône confluence on April 12^{th} 2023. "RA" for "Rhône upstream" and "SA" for "Saône upstream".

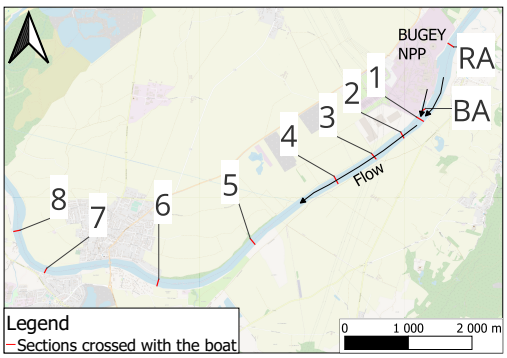

(b) Figure 2.b: Measurement cross-sections on Rhône-Bugey outflow on October 10^{th} 2023. "RA" for "Rhône upstream" and "BA" for "Bugey upstream"

2.3 *Data processing*

Each point of conductivity/temperature mesured by the HOBO probes is associated with one point of pressure measured by a DIVER probe and is connected through the time to the DGPS position. Assuming that the rope underneath the boat is vertical, the pressure permits to estimate the measurement depth and the synchronization with the DGPS permits to estimate the horizontal position of the probe. After that, a binning permits to plot a map of temperatures and conductivity over each section. An interpolation, and a vertical extrapolation to the bottom and the free-surface in the blind areas finally lead to a full visualisation of the mixing interface in each cross-section. Besides, secondary currents vectors displaying is possible by coupling the Python code with QRevInt software (Mueller 2020) and MAP extension now in QRevInt. The density of both inflows is calculated from IAPWS 95 formula (for the Thermodynamic Properties of Ordinary Water Substance for General and Scientific Use) from the averaged temperatures of each tributary, and thus provides a density ratio:

$$\Delta\rho* = \frac{\rho_1 - \rho_2}{\rho_1} \tag{3}$$

With ρ_1 and ρ_2 densities of lighter and heavier rivers. Finally, the velocity ratio between both inflows is calculated as VR = U_{trib} / U_{main} (with U: mean velocity, and $trib$ and $main$, the tributary and the main river).

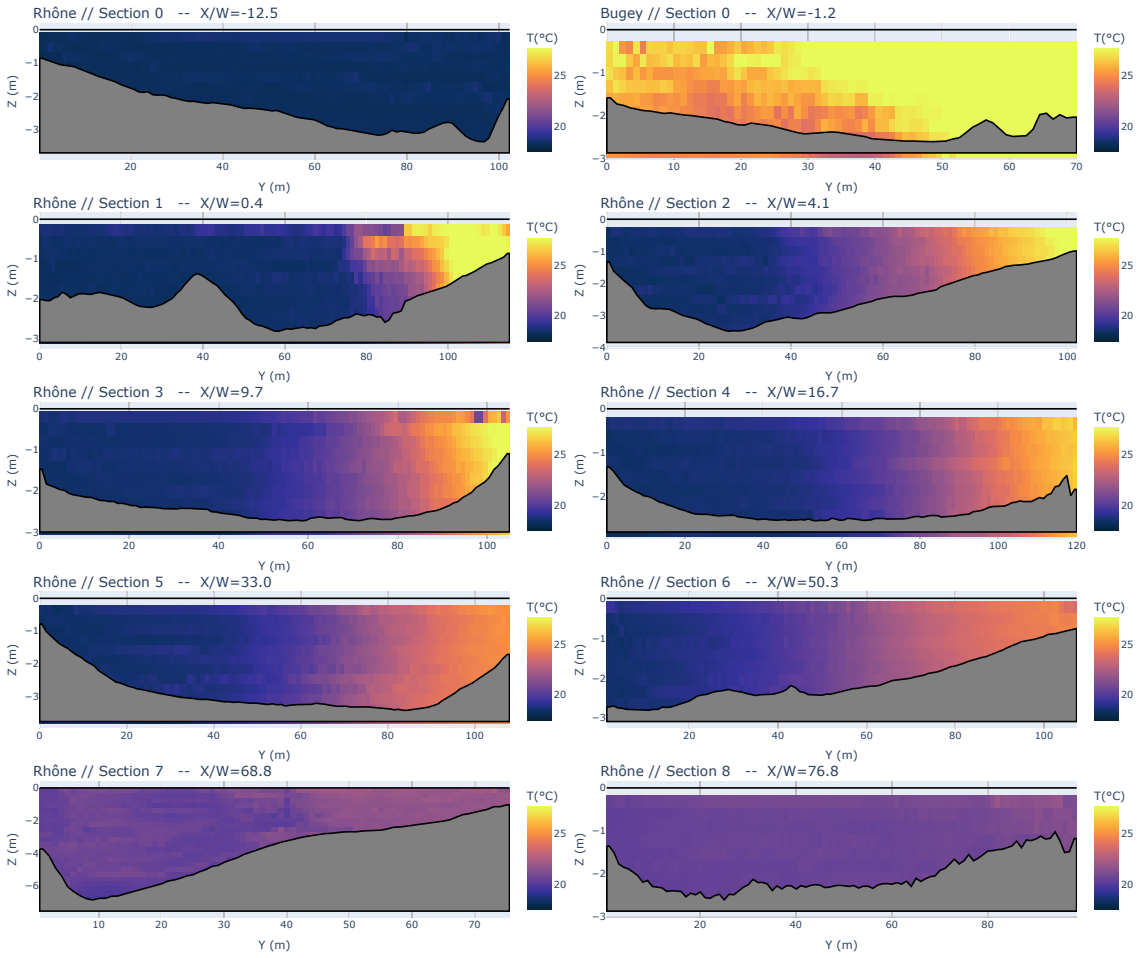

Figure 3.: Distribution of water temperatures throughout cross-sections upstream and downstream of the Rhône-Bugey confluence on 10 th October 2023

3 RESULTS

3.1 *One case of a mixing dominated by turbulent diffusion*

The first case was measured downstream the Bugey NPP outflow. During this field experiment, the depth of the Rhône River was about 1 to 5 meters, depending on the section. The discharge of the Rhône River was 258 m^3/s, and 47 m^3/s for the thermal outflow of the Bugey NPP. The density of the Rhône River was 998.41 kg/m^3, and 996.38 kg/m^3 for the other tributary. The velocity was 0.5 m/s for the Bugey NPP outflow and 1.12 m/s for the Rhône River. The velocity ratio was then 0.45 (see table 1). The temperature difference of around 10°C is clearly visible on the figure 3, and $\Delta\rho*$ =0.0018. On section 1, the mixing interface is slightly tilted, and, on the surface, a fraction of the thermal outflow tends to go toward the left bank. From section 2 and further downstream, the mixing interface is horizontal, and the warmer water remains along the right bank over the entire height, without noticeable gravity current, despite a large difference in density. The mixing process seems to be dominated by the turbulent diffusion induced by the shear due to the velocity difference between both flows. The thickness of the interface (defined as the intermediate temperature zone between the upstream values of the Bugey NPP outflow and the Rhône River) increases moving downstream until reaching full mixing in section 8.

3.2 *One case of a mixing dominated by dispersion*

The second case was measured on April 2023 at Rhône-Saône confluence. The discharge of the Rhône River was 407 m^3/s, and 330 m^3/s for the Saône River. The Rhône River density was 999.322 kg/m^3, and it was 999.472 kg/m^3 for the Saône River; so the density ratio was 0.00015. The velocity of the Saône River was 0.42 m/s and 0.26 m/s for the Rhône River, so that $VR = 1.62$. This confluence has a 10 to 15 meters depth approximately, depending on the section. The

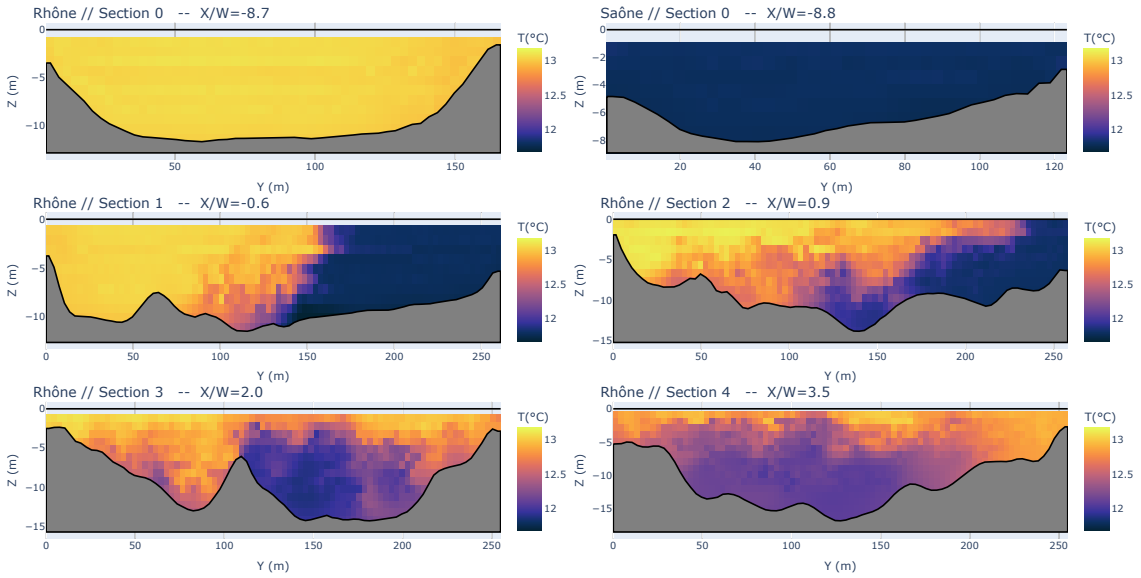

Figure 4.: Distribution of water temperatures throughout cross-sections upstream and downstream of the Rhône-Saône confluence on 12 th April 2023

evolution of mixing downstream of the river confluence is presented in figure 4. In this case, the Saône River, passes under the lighter Rhône River with a gravity current that starts immediately a few meters downstream of the apex from section number 1, at $X/W = 0.6$. This current progresses at the bottom toward the Rhône bank at section 2, like in a lock-exchange flow (Cheng and Constantinescu 2022), and tends to become horizontal. At section 3, the gravity current seems trapped at the bottom of the river because of a great rise in bathymetry. Finally, at the distance downstream of the apex ($X/W = 3.5$), on section 4, the heavier water seems to have completely spread out across the channel width and the temperature of the river decreases from the surface to the bottom over the whole cross-section.

3.3 *Application of the dimensionless numbers*

The Gamma parameter and the Densimetric Froude numbers were computed for the 8 field experiments to evaluate the dominant type of mixing with the qualitative description method for instance (Table 1).

The Rhône-Saône confluence mixing was dominated by a density gradient for the 5 corresponding field experiments. These gravity currents were inverted depending on the season. In December and April, the Saône River was heavier than the Rhône River due to their temperature difference and passed under the Rhône River. The opposite happened in July and October. In all cases on this site, FrD was lower than 2.5, and γ greater than 3.

For the two cases of Rhône-Arve confluence, the density ratio was 10 times lower than Rhône-Saône confluence, and the velocity ratio was about equal to 2, which corresponds to the highest value measured on all field experiments. Data processing revealed a mixing dominated by turbulent diffusion with a large distance necessary for a good mixing ($X/W = 77$), on these two cases. FrD was always greater than 5, and γ less than 1.5. These values differ from the treshold values for a mixing dominated by turbulent diffusion for γ corresponding to < 1 (White and Helfrich 2013), and the treshold value for $FrD > 7$ (Duguay et al. 2022b), or > 10 (Horna-Munoz et al. 2020) , but our values are close to these tresholds.

Finally, the latest data comes from the confluence between the Rhône River, and the thermal outflow of the Bugey NPP. It is important to notice that the depth was less than 2 meters in some locations near the confluence apex. The discharge water from the NPP was 10°C warmer than the Rhône River immediately at the appex. This difference induced a density ratio of 0.0019, which corresponds to a value 2 at 10 times greater than Rhône-Saône confluence, and approximately 25 time greater than Rhône-Arve confluence. In this case the mixing was clearly dominated by the turbulent diffusion (3), and the mixing interface was vertical. The distance necessary for a good mixing could not be reached due to the next confluence with the Ain River downstream. In this

case, FrD= 5.26, and γ= 1.26. These values approach those of the Rhône-Arve confluence having a mixture dominated by turbulent diffusion. Even if the difference in velocity is significant, it is also possible that the low water height blocks the dispersion process and generates a large length necessary for a good mixing.

Confluence location	Date	Depth [m]	Width [m]	Mean Velocity downstream [m/s]	Density ratio Δρ*	Velocity ratio VR= U_{trib}/U_{main}	Momentum ratio (M*)	Densimetric Froude number (FrD)	Gamma parameter (Ɣ)	Gravity current?
Rhône-Saône, Lyon, France	19/12/2022	9,31	264,3	0,334	0,00024	1,02	0,54	2,25	106,02	yes
	12/04/2023	9,58	261,8	0,294	0,00015	1,62	1,31	2,47	3,67	yes
	13/07/2023	9,90	264,95	0,231	0,00070	0,32	0,06	0,89	5,74	yes
	21/07/2023	9,33	264,83	0,238	0,00091	0,15	0,01	0,83	4,88	yes
	05/10/2023	9,38	265,67	0,132	0,00031	0,17	0,01	0,78	5,11	yes
Rhône-Arve, Geneva, Switzerland	04/01/2023	6	97,42	1,043	0,00007	0,57	0,14	16,18	0,77	no
	11/04/2023	6	95,74	0,397	0,00009	2,01	1,13	5,52	1,48	no
Rhône-CNPE Bugey, Saint-Vulbas, France	10/10/2023	2,32	119,85	1,094	0,0018925	0,45	0,08	5,26	1,66	no

Table 1. Results of dimensionless numbers for the mixing characterization on 8 field experiments at Rhône-Saône, Rhône-Arve confluence and Bugey NPP outflow

4 DISCUSSION / CONCLUSION

This study applied a method to visualize the water mixing at confluences, with 8 field experiments measured at 3 sites. Two dimensionless numbers characterizing the weight of density effects, have been estimated for each case and summarized in Table 1. First, at the Rhône-Saône confluence, the data showed a good correlation between the dominating mixing processes and the values of the Densimetric Froude number and Gamma parameter: all values of the FrD parameter were less than 3 and all values of gamma parameter greater than 3, with the presence of a stong density current cells. These numbers thus seem to be good candidates to predict the relative weight of dispersion affected by a density current and turbulent diffusion. But it is possible that this gravity current is caused by the difference in bathymetry between the two rivers, and the weight of this contribution remains poorly understood. Seconde, at the Rhône-Arve confluence, the mixing was dominated by turbulent diffusion with all values of FrD exceeding 4. This threshold slightly differs from those proposed in the literature: $FrD > 7$ (Duguay et al. 2022b), or > 10 (Horna-Munoz et al. 2020). The exact threshold value for FrD in not yet completely clear. Besides, γ was close to unity, but never smaller. This low value is in agreement with the value of unity proposed in the literature data (White and Helfrich 2013) even the exact threshold value is, once more, to be clarified. Third, for the Bugey nuclear power plant outflow, the mixing was dominated by the turbulent diffusion, even with a value of γ = 1.66, slightly exceeding the threshold value of 1.

In conclusion, the two dimensionless numbers appear to be good candidates for assessing the relative weight of dispersion and turbulent diffusion processes contributing to the water mixing at river confluences, but more precise treshold values need to be quantified. Still, many other parameters can affect the mixing, like the junction angle (Riley et al. 2015), the bed morphology (Biron et al. 1993) and the momentum ratio. The values of these dimensionless numbers can also vary greatly, depending on the exact definition of each term involved (Duguay et al. 2023). A consensus remains to be established to avoid differences of interpretation between authors. And, finally, the definition of a ”strong” or ”weak” density effect remains unclear. A new methodology will be applied shortly to quantify the relative weight of dispersion and turbulent diffusion on the mixing process.

REFERENCES

ASN. 2022. L'ASN tire le retour d'expérience des décisions prises pendant la canicule de l'été 2022: *https://www.asn.fr/l-asn-informe/actualites/l-asn-tire-le-retour-d-experience-des-decisions-prises-pendant-la-canicule-de-l-ete-2022.*

Biron, P., Roy, A G., Best, J L., & Boyer, C. J. 1993. Bed Morphology and Sedimentology at the Confluence of Unequal Depth Channels. In: *Geomorphology* 8.2, pp. 115–129.

Cheng, Z., & Constantinescu, G. 2019. Stratification Effects on Hydrodynamics and Mixing at a River Confluence with Discordant Bed. In: *Environmental Fluid Mechanics* 20.4, pp. 843–872.

Cheng, Z., & Constantinescu, G. 2022. Shallow Mixing Interfaces between Parallel Streams of Unequal Densities". In: *Journal of Fluid Mechanics* 945, A2.

Dong, C., MinQuan F., HaiXiao J., & XiaoGe, D. 2023. Density Differences Affect the Mixing Process of Pollutants in The River Confluence Area. In: *CLEAN – Soil, Air, Water* p. 2200224.

Duguay, J., Biron, P., & Lacey, J. 2023. Density Effects on Streamwise-Orientated Vorticity at River Confluences: A Laboratory Investigation. In: *Journal of Fluid Mechanics* 973, A7.

Duguay, J., Biron, P., & Lacey, J. 2022a. Aerial Observations and Numerical Simulations Confirm Density-Driven Streamwise Vortices at a River Confluence. In: *Water Resources Research* 58.7.

Duguay, J., Biron, P., & Lacey, J. 2022b. Impact of Density Gradients on the Secondary Flow Structure of a River Confluence. In: *Water Resources Research* 58.10.

Fischer, H. B. 1979. Mixing in Inland and Coastal Waters. In: *Academic Press*.

Gualtieri, C., Ianniruberto, M., & Filizola, N. 2019. On the Mixing of Rivers with a Difference in Density: The Case of the Negro/Solim˜oes Confluence, Brazil. In: *Journal of Hydrology* 578, p. 124029.

Herrero, H. S., Dìaz Lozada, J. M., Garcìa, C. M., Szupiany, R. N., Best, J., & Pagot, M. 2018. The Influence of Tributary Flow Density Differences on the Hydrodynamic Behavior of a Confluent Meander Bend and Implications for Flow Mixing. In: *Geomorphology* 304, pp. 99–112.

Horna-Munoz, D., Constantinescu, G., Rhoads, B., Lewis, Q., & Sukhodolov, A. 2020. Density Effects at a Concordant Bed Natural River Confluence. In: *Water Resources Research* 56.4.

Jiang, C., Constantinescu, G., Yuan, S., & Tang, H. 2022. Flow Hydrodynamics, Density Contrast Effects and Mixing at the Confluence between the Yangtze River and the Poyang Lake Channel. In: *Environmental Fluid Mechanics* 23.2, pp. 229–257.

Lane, S. N., Parsons, D. R., Best, J. L., Orfeo, O., Kostaschuk, R. A., & Hardy, R. J. 2008. Causes of Rapid Mixing at a Junction of Two Large Rivers: Rìo Paranà and Rìo Paraguay, Argentina. In: *Journal of Geophysical Research: Earth Surface* 113.F2.

Mueller, D. S. 2020. QRev. U.S. Geological Survey.

Pouchoulin, S., Le Coz, J., Mignot, E., Gond, L., & Riviere, N. 2020. Predicting Transverse Mixing Efficiency Downstream of a River Confluence". In: *Water Resources Research* 56.10.

Ramòn, C. L., Hoyer, A. B., Armengol, J., Dolz, J., & Rueda, F. J. 2013. Mixing and Circulation at the Confluence of Two Rivers Entering a Meandering Reservoir. In: *Water Resources Research* 49.3, pp. 1429–1445.

Rhoads, B. L. 2020. River Dynamics: Geomorphology to Support Management. In: *Cambridge University Press*.

Riley, J D., Rhoads, B. L., Parsons, D. R., & Johnson, K. 2015. Influence of Junction Angle on Three-Dimensional Flow Structure and Bed Morphology at Confluent Meander Bends during Different Hydrological Conditions. In: *Earth Surface Processes and Landforms* 40.2, pp. 252–271.

Rutherford, J. C. 1994. River Mixing. In: *Wiley*

White, B. L. & Helfrich, K. R. 2013. Rapid Gravitational Adjustment of Horizontal Shear Flows. In: *Journal of Fluid Mechanics* 721, pp. 86–117.

Xu, L., Yuan, S., Hongwu T., Jiajian Q., Xiao, Y., Whittaker, C., & Gualtieri, C. 2022. Mixing Dynamics at the Large Confluence Between the Yangtze River and Poyang Lake. In: *Water Resources Research* 58.11.